Dinuclear platinum(II) complexes emitting through TADF: new ligand design to minimise aggregation and the S_1–T_1 energy gap†

Piotr Pander, ‡*[a,b] Yana M. Dikova, ‡[c] Emma V. Puttock [c] and J. A. Gareth Williams*[c]

E-mail: piotr.pander@polsl.pl

Dinuclear platinum(II) complexes of a new, ditopic, bis-tridentate *NCN*–*NCN*-coordinating ligand, appended with four mesityl groups, are reported. The high radiative rate constants and correspondingly efficient luminescence of the complexes involves thermally activated delayed fluorescence (TADF), thanks to a near-zero energy gap between the S_1 and T_1 states. The mesityl groups also serve to hinder the aggregation that was detrimental to electroluminescence efficiency in previous studies, allowing a ~4 fold increase in OLED efficiency to be achieved (*i.e.* from 2.3% previously to 10% in this work). Oxidation of one of the Pt(II) complexes led to a dinuclear Pt(IV) complex of unprecedented structure.

Introduction

Organoplatinum(II) complexes are widely used as the luminophore or sensitizer in diverse applications, often complementing their iridium(III) counterparts.[1–3] Important uses include bioimaging,[4–9] photodynamic therapy,[10] photocatalysis,[11–14] and organic light-emitting diodes (OLEDs).[15–18] The luminescence displayed by such complexes is normally considered phosphorescence, whereby the high spin-orbit coupling associated with the heavy metal relaxes the spin selection rule, accelerating the rate of the otherwise forbidden $T_1 \rightarrow S_0$ process.[19,20] However, recent findings by some of the present authors have revealed that another mechanism may be at work in at least some such complexes, involving thermally activated delayed fluorescence (TADF).[21–23] Dinuclear Pt(II) complexes of ditopic ligands featuring a pyrimidine bridge were found to have a small energy gap ΔE_{ST} between the lowest singlet S_1 and triplet T_1 excited states.[22] It leads to a shortening of the decay lifetime by thermal activation of T_1 to S_1 and subsequent emission through the allowed $S_1 \rightarrow S_0$ transition (*i.e.*, following the TADF model).[24,25] A similar phenomenon has since been observed by others in a mononuclear Pt(II) complex,[26] and the future discovery of many further examples seems likely.

In the present work, we took our original ligand design and appended it with four 2,4,6-trimethylphenyl (mesityl) groups, with a view to improving the solubility of the resulting complex and reducing aggregation. We also show how this seemingly otherwise insignificant structural change leads to a reduction in ΔE_{ST}, which in turn enhances the TADF contribution to emission and substantially improves performance.

Results and discussion

Synthesis

The new ditopic *NCN*–*NCN* proligand H_2L (compound **4** in **Scheme 1**) was prepared by a sequence of Pd-catalysed cross-coupling reactions from readily obtainable starting materials; full experimental details and the characterisation of new compounds are given in the Supporting Information. Compound H_2L was platinated using K_2PtCl_4 in acetic acid to give the dinuclear complex $L(Pt–Cl)_2$ (**5**), from which the iodo derivative $L(Pt–I)_2$ (**6**) was prepared by metathesis of the monodentate ligand upon treatment with $Ag(SO_3CF_3)$ followed by KI. We were unable to obtain crystals of **5** or **6** of sufficient quality for an X-ray diffraction study, but the oxidation of **5** with $PhICl_2$ led cleanly to $L(Pt–Cl_3)_2$ (**7**), a dinuclear Pt(IV) complex of unprecedented structure that was amenable to crystallography. Although the thrust of the current work is the Pt(II) systems, there is growing interest in the less widely explored +4 oxidation state,[27,28] and **7** represents an interesting structure in that context for future elaboration by replacement of the chloride ligands.[29] Here, it offers insight into the likely structures of **5** and **6**. The structure (**Fig. 1**) shows the two Pt centres in very similar pseudo-octahedral environments, each bound to an *NCN* unit with three chlorides completing the coordination sphere. The

[a] *Faculty of Chemistry, Silesian University of Technology, M. Strzody 9, 44-100 Gliwice, Poland*
[b] *Centre for Organic and Nanohybrid Electronics, Silesian University of Technology, Konarskiego 22B, 44-100 Gliwice, Poland*
[c] *Department of Chemistry, Durham University, South Road, Durham, DH1 3LE, UK*

† Electronic Supplementary Information (ESI) available: Synthetic details and characterisation of new materials; X-ray diffraction and crystal data; further information on the equipment and methods for theory, photophysical characterisation, and OLED devices. CCDC 2365020.

‡ These authors contributed equally to the experimental work.

torsion angles between the mesityl and phenyl rings are in the range 69 ± 3° and, between the pyridyl and mesityl rings, 69 ± 5°. These angles are a little less than that of 80° in the related mesityl-appended *NCHN* proligand,[30] suggesting a slightly greater degree of conjugation across the rings upon complexation, attenuating the steric preference for orthogonality.

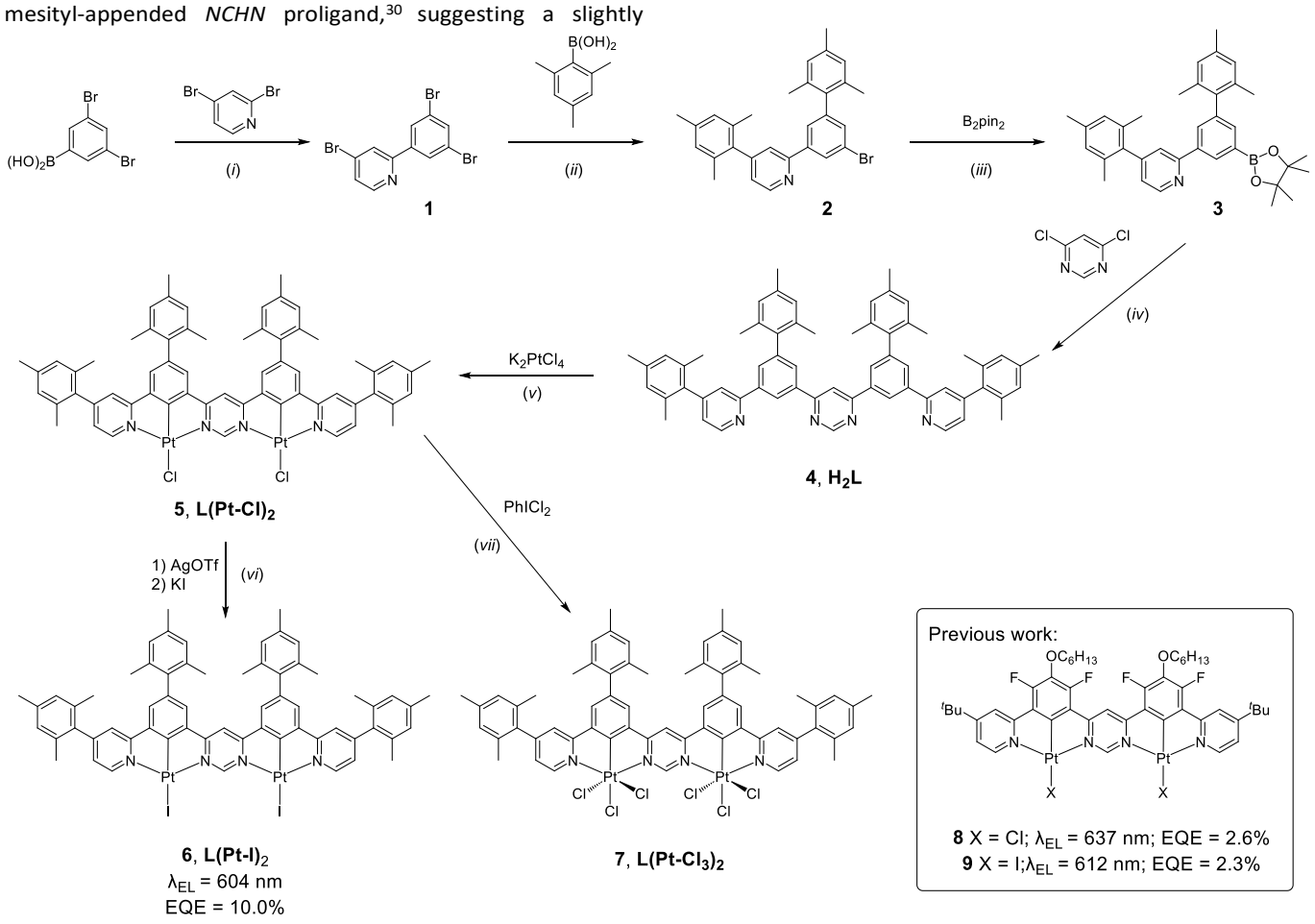

Scheme 1 Synthetic procedure for complexes **5**, **6** and **7**: (*i*) toluene/EtOH/H_2O (2:1:1 v/v), $Pd(PPh_3)_4$, Na_2CO_3, 70°C (2 h) → 90°C (18 h), 35%; (*ii*) toluene, $Pd(PPh_3)_4$, Cs_2CO_3, 90°C (18 h), 67%; (*iii*) dioxane, $Pd(dppf)Cl_2{\cdot}CH_2Cl_2$, KOAc , 90°C (18 h); (*iv*) toluene, $Pd(PPh_3)_4$, Cs_2CO_3, 90°C (18 h), 35%; (*v*) AcOH, reflux, 65%; (*vi*) step 1: acetone, RT (1.5 h); step 2: RT (2 h); 67%; (*vii*) $CHCl_3$, RT (18 h), 78%. Inset: the previously studied complexes **8** and **9** incorporating a related *NCN*–*NCN*-coordinating ligand.

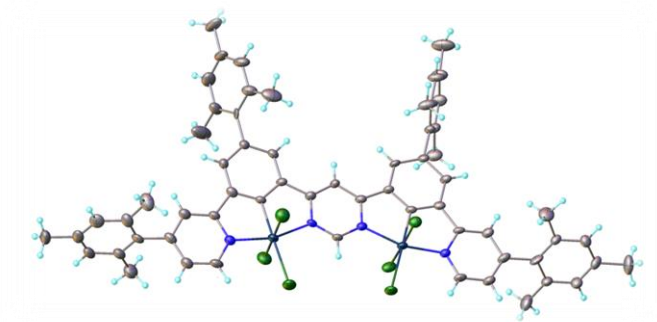

Fig. 1 The molecular structure of the dinuclear Pt(IV) complex $L(Pt–Cl_3)_2$, **7**.

DFT and TD-DFT calculations

The excited states in **5** and **6** were probed by DFT/TD-DFT at the B3LYP/def2-SVP level of theory using ORCA 5.0.3,[31,32] and by quasi-degenerate perturbation theory (QDPT).[33,34] The optimised T_1 geometries (**Fig. 2**) show torsions between the plane of the *NCN*–*NCN* unit and the pendent mesityl rings that are similar to those observed experimentally in the Pt(IV) complex (atomic coordinates for T_1 and S_0 are given as separate Supporting files). The mesityl groups thus form a congested shield around the complex, which is expected to inhibit intermolecular interactions between *NCN*–*NCN* planes.

The frontier molecular orbital isosurfaces of **5** and **6** (**Fig. 2**) resemble those of **8** and **9**,[22,23] with the LUMO distributed over the pyrimidine linker and the neighbouring benzene rings, but also including a small admixture of *d* orbitals from both Pt(II) centres. The HOMO comprises *d* orbitals of both the Pt centres and *p* orbitals of their respective monodentate halide ligands. For **6**, there are no significant contributions from other parts of the molecule, such that the degree of HOMO-LUMO overlap is small. In **5,** the HOMO includes additional contributions from π orbitals of the organic ligand, which serves to increase the HOMO–LUMO overlap. In both complexes, the S_1 and T_1 are associated mainly with the HOMO→LUMO transition, and thus

may be classed as MXLCT or metal-halogen-to-ligand charge-transfer in character.

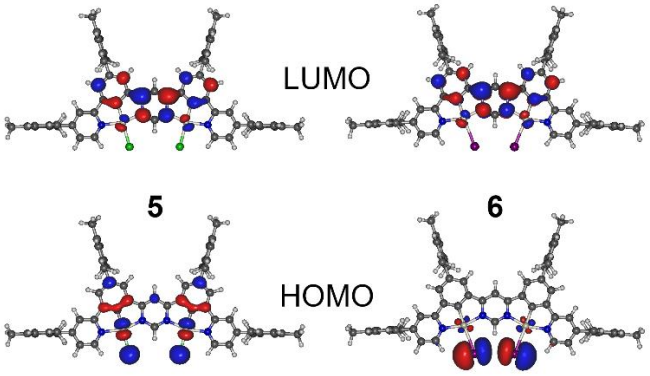

Fig. 2 HOMO and LUMO of complexes **5** and **6** calculated using the B3LYP/def2-SVP//B3LYP/def2-TZVP level of theory.

When spin-orbit coupling (SOC) is included in the calculations, excited states of predominantly triplet or singlet nature are identified (Fig. S4.1, Tables S4.1 and S4.2). The lowest triplet state splits into three closely separated levels, the separation between the first and third, ΔE_{1-3}, being the zero-field splitting (ZFS). Values of 2 meV (13 cm^{-1}) and 15 meV (119 cm^{-1}) are calculated for **5** and **6** respectively. In **5**, state 7 is the first excited state with predominant singlet character (68%; states 4–6 are associated with T_2); thus $\Delta E_{ST} = \Delta E_{1-7}$, which is calculated to be 291 meV (2345 cm^{-1}). For **6**, the first predominantly singlet excited state (81.4%) is state 4, and $\Delta E_{ST} = \Delta E_{1-4}$ = 19 meV (149 cm^{-1}). The trend to smaller ΔE_{ST} upon changing X from Cl to I is consistent with that observed previously for **8** and **9**.

Solution-state photophysics

The solvent of choice for photophysical measurements is toluene (PhMe) (based on **9** having previously shown the highest radiative rate in this solvent[23]). Here, we studied **6** in toluene, but **5** has poorer solubility and intermolecular interactions suppress its emission leading to a lower Φ_{PL}. The full characterisation of **5** was therefore performed in chlorobenzene (PhCl), where such interactions were essentially absent.[‡,¶] There is substantial overlap between the photoluminescence (PL) spectrum and the lowest-energy absorption band in both complexes (**Fig. 3**) – a clear indication that the PL originates not from the lowest-energy T_1 state but rather from a higher state, and a strong clue for the involvement of TADF.

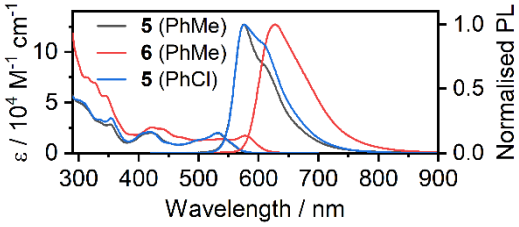

Fig. 3 Absorption and photoluminescence spectra of **5** and **6** in dilute (c = 10^{-5} M) toluene (PhMe) and (for **5**) chlorobenzene (PhCl) solutions.[‡,¶]

The PL spectrum of **6** is very similar to that of the analogous complex **9** (λ_{max}^{PL} = 627 and 628 nm respectively),[23] but the emission spectrum of **5** (λ_{max}^{PL} = 576 nm) is drastically different from that of **8** (λ_{max}^{PL} = 617 nm), **Fig. 4**. The difference between the PL of **5** and **8** in chlorobenzene can be attributed to a significantly smaller ΔE_{ST} in the former with TADF dominating the spectrum at RT as opposed to **8** with phosphorescence being the dominant component. As the PL onsets are similar in either case, the S_1 energy is lilely comparable in both complexes, but the structural differences between the two luminophores leads to a higher T_1 energy in **5** (Table S5.2).

The PL spectra of the complexes in solution are sensitive to temperature (Figs S5.1 and S5.2), in line with the TADF mechanism. For **5** in PhCl, the interplay between phosphorescence and TADF at intermediate temperatures is evident, as in **8**. For **6**, however, the PL spectrum blue shifts very slightly at lower temperatures, indicating a visible influence of suppressed molecular motion. Even at 160 K, there is no evidence of phosphorescence (in stark contrast to the behaviour of **9** for example), suggesting that ΔE_{ST} in **6** is very small indeed, with TADF consequently predominating even at low temperatures.

Complexes **5** and **6** display unusually large radiative decay rate constants k_r for platinum(II) complexes: τ = 0.34 µs, Φ_{PL} = 0.11, $k_r = 3.3 \times 10^5$ s^{-1} for **5** in PhMe [τ = 2.1 µs, Φ_{PL} = 0.45, $k_r = 2.1 \times 10^5$ s^{-1} in PhCl]; τ = 0.40 µs, Φ_{PL} = 0.23, $k_r = 5.7 \times 10^5$ s^{-1} for **6** in PhMe.[§] The k_r values are significantly higher than for **8** and **9** (Table S5.1), suggesting more efficient TADF. We use the method of Strickler and Berg[35] to estimate the *singlet-state* radiative rate constants k_r^S and $f(S_1 \rightarrow S_0)$ oscillator strengths, from the lowest energy absorption bands.[36,37] For **5** in PhCl, $k_r^S = 1.8 \times 10^7$ s^{-1} and $f(S_1 \rightarrow S_0)$ = 0.039; corresponding values for **6** in PhMe are 1.1×10^7 s^{-1} and 0.029. The values are two orders of magnitude higher than the experimental values, showing (as expected) that the emission is not fluorescence, but rather pointing to the likely involvement of TADF.

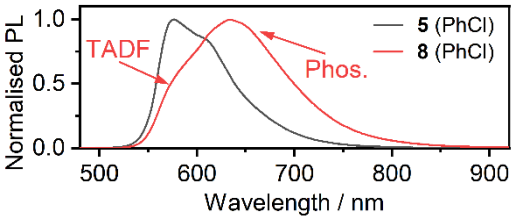

Fig. 4 Comparison of photoluminescence spectra of compounds **5** and **8** recorded in dilute PhCl.

Solid-state photophysics

More conclusive evidence of a TADF mechanism comes from the temperature dependence of the complexes' PL spectra in a dilute polystyrene (PS) film, over the range 295 – 80 K (**Fig. 5**). The spectra display a clear change, shifting to the red as the temperature decreases, from which it is apparent that TADF dominates at 295 K, while phosphorescence from the lower-energy T_1 state dominates at 80 K. The evolution of the spectra correlates with a change in the radiative lifetime (**Fig. 6**, Figs

S5.4 and S5.5). Fitting of the lifetime data of **6** to an established Boltzmann-based expression (Equation S2) gives a natural fluorescence lifetime $\tau_0 \approx 32$ ns, phosphorescence lifetime $\tau_{PH} \approx 13$ µs, and $\Delta E_{ST} \approx 66$ meV, not dissimilar to the value calculated by TD-DFT. The k_r^S figures for both complexes (~10^7 s^{-1}) are in good agreement with the estimates obtained using the Strickler-Berg method. It is striking that the radiative lifetime at 295 K is an order of magnitude shorter than at 80 K thanks to the involvement of TADF, underscoring how TADF can benefit Pt(II) complexes despite the heavy atom effect that might otherwise be expected to funnel emission through phosphorescence.

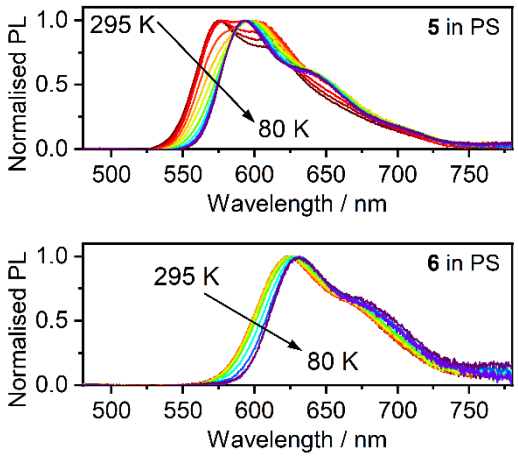

Fig. 5 PL spectra of **5** and **6** in polystyrene dispersion (c = 0.2% w/w) over the temperature range indicated.

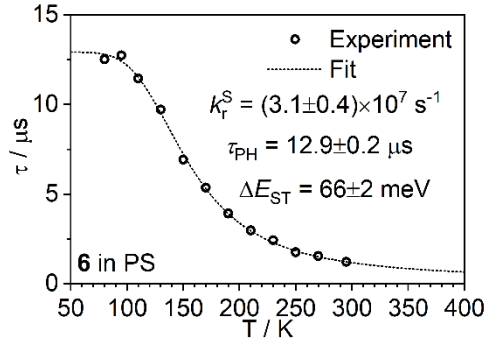

Fig. 6 Variation of the PL decay lifetime τ of **6** as a function of temperature *T*.

OLED devices

Owing to the good PL properties of **6** and its low susceptibility to aggregative quenching (in contrast to **5**), it was tested as an emitter in a solution-processed organic light-emitting diode (OLED). Three pairs of device architectures (Tables S6.1 and S6.3) were trialled to optimise the efficiency: Devs 1, 3, and 5 at 3% w/w loading of the complex in the host, and Devs 2, 4, and 6 at 5%, to probe the effect of concentration. The pair of devices 1 and 2 use a simple structure with a relatively thick TCTA:PO-T2T host emissive layer.[38] Devices 3 and 4 feature a mCP:PO-T2T host. Devices 5 and 6 employ a mCP:PBD host with a poly(vinyl-carbazole) hole-transporting and electron-blocking layer (as previously used with **9** and hence serving as a reference[23]). The OLED data are presented in **Fig. 7**, Figures S6.1-S6.8 and Table S6.1.

Comparison of Devices 5 and 6 with those reported previously using **9** shows that the use of the new complex leads to a ~4-fold higher EQE (up to 10%) than complex **9**, and a ~2-4-fold higher luminance (up to 8700 cd m^{-2}). Although several factors may have contributed to this result, the main one appears to be suppression of emitter aggregation in the solid state by the mesityl substituents. This effect can be identified from a comparison of the respective EL spectra (**Figure 8**). Despite identical emitter loading and OLED structure, Device 6 displays a visibly narrower EL spectrum, lacking the long wavelength tail > 700 nm that the previously reported Device 7 shows (using complex **9**). That tail is due to dimeric or oligomeric species formed through aggregation; it is detrimental both to the overall OLED EQE and to colour purity.[#] Thus, the encumbered molecular design is successful in promoting efficiency in OLEDs using dinuclear Pt(II) TADF emitters.

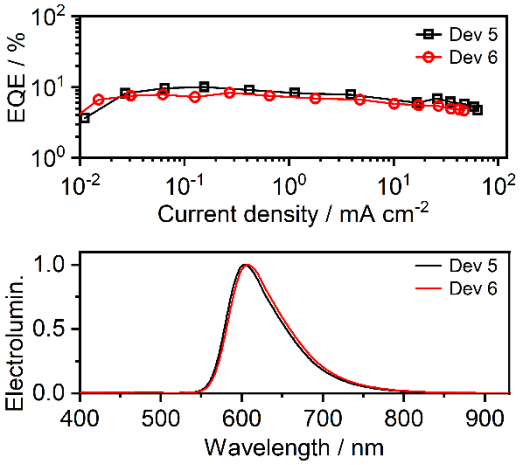

Fig. 7 Characteristics of OLEDs 5 and 6: (*top*) External quantum efficiency (EQE); (*bottom*) EL spectra.

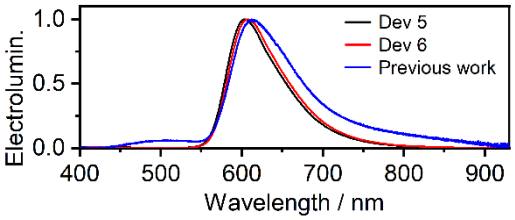

Fig. 8 Comparison of the EL spectra of OLEDs 5 and 6 with the EL spectrum of OLED 7 (using complex **9**) from previous work.[23]

Conclusions

In conclusion, the design of ligand **4** – featuring a ditopic *NCN*–*NCN* core decorated with four mesityl units – successfully limits aggregation of complex **6**, inhibiting the detrimental effect on EL in an OLED. Complex **6** is highly soluble in toluene and other solvents and displays a lower susceptibility to aggregation in the solid state than the previously reported complex **9**. The presence of the hexyl chains and *t*-butyl substituents in **9** are

insufficient to impede intermolecular interactions, whereas the mesityl groups of **6** do so. The solution-processed OLEDs reach an EQE of 10% with a maximum luminance of 5400 cd m^{-2} (Dev 5), or EQE of 9.2% with a maximum luminance of 8700 cd m^{-2} (Dev 3). These figures exceed by ~4-fold the values reported for the structurally similar complex **9**, and are the highest values reported for a TADF-based Pt(II) emitter. Moreover, the use of ligand **4** also leads to a significant reduction of the ΔE_{ST} (*e.g.*, to 0.07 eV in **5** in PS, compared to 0.20 eV reported for complex **8**). This is achieved by increasing the T_1 energy in complex **5**.

The high solubility attained using ligand **4** could also be exploited to oxidise the dinuclear Pt(II) **5** complex to the corresponding dinuclear Pt(IV) complex **7**. Analogous attempts to prepare such materials from related, less substituted *NCN*–*NCN* ligands have led to intractable mixtures, probably due to poor solubility.

In summary, this study has shown how modifying the design of rigid, ditopic, bis-tridentate ligands can simultaneously lead to improvements in several properties of the corresponding Pt_2 complexes, including enhanced solubility, lower propensity to aggregation, and a reduction in ΔE_{ST} that serves to accelerate radiative decay through TADF. We expect TADF to be implicated in the emission of many other 3rd row phosphors and that these findings will help inform the future design of such molecules.

Author Contributions

P. P. – Conceptualization, Funding acquisition, Project administration, Formal analysis, Investigation (synthesis, photophysics, OLED devices, computations), Visualization, Writing – original draft, Writing – review & editing; Y. M. D. – Investigation (synthesis), Writing – review & editing; E. V. P. – Conceptualization , Investigation (synthesis), Writing – review & editing; J. A. G. W. – Conceptualization, Funding acquisition, Resources, Project administration, Supervision, Writing – original draft, Writing - review & editing.

Conflicts of interest

There are no conflicts of interest to declare.

Data availability

Our supporting research data is available from the Durham Research Online DATAsets Archive (DRO-DATA) open data repository. DOI: XXXXXXXX.

Acknowledgments

We thank Dr Dmitry Yufit for determining the structure of compound **7** through X-ray diffraction. P.P. thanks the National Science Centre, Poland for funding under grant no. 2022/47/D/ST4/01496, and the Rector's pro-quality grant, Silesian University of Technology, Poland, grant no: 04/040/RGJ24/0279. E.V.P. and J.A.G.W. acknowledge funding from EPRSC (grant ref. EP/S012788/1). Y.M.D. thanks Durham University Chemistry for partial support of a PhD studentship. P.P. thanks Dr F. B. Dias and Prof. A. P. Monkman for access to facilities. This work made use of the Hamilton High Performance Computing Service of Durham University.

Notes and references

‡ A slight difference between the PL spectra of **5** in toluene and chlorobenzene can be ascribed to a variation in the ΔE_{ST}, in line with the previous report of complex **8**.[22] Here, **5** displays a larger ΔE_{ST} in the higher polarity chlorobenzene than in toluene, leading to a visible phosphorescence contribution in chlorobenzene, manifest on the low-energy side of the spectrum.
¶ Complex **7** does not show any detectable emission, as expected based on earlier studies.[28,29] The absorption spectrum of **7** is included in the Supporting Information for completeness (Figure S5.3).
§ k_r is estimated from the lifetime and quantum yield, assuming unit population of the emissive state, where $k_r = \Phi/\tau$. The quoted τ and Φ values were measured in deoxygenated solution at 295 K.
# Some deleterious interactions nevertheless remain, as the 3%-loaded devices are generally more efficient than the 5% devices, a trend also widely observed with, for example, Ir(III) emitters.

1 P. L. dos Santos, P. Stachelek, Y. Takeda and P. H. Pander, *Mater. Chem. Front.*, , DOI:10.1039/D3QM01067H.
2 K. Li, G. S. Ming Tong, Q. Wan, G. Cheng, W. Tong, W.-H. Ang, W.-L. Kwong and C. Che, *Chem. Sci.*, 2016, **7**, 1653–1673.
3 B. Ma, P. I. Djurovich, S. Garon, B. Alleyne and M. E. Thompson, *Adv. Funct. Mater.*, 2006, **16**, 2438–2446.
4 W. A. Tarran, G. R. Freeman, L. Murphy, A. M. Benham, R. Kataky and J. A. G. Williams, *Inorg. Chem.*, 2014, **53**, 5738–5749.
5 M. Mauro, A. Aliprandi, D. Septiadi, N. S. Kehr and L. De Cola, *Chem. Soc. Rev.*, 2014, **43**, 4144–4166.
6 C.-K. Koo, K.-L. Wong, C. W.-Y. Man, Y.-W. Lam, L. K.-Y. So, H.-L. Tam, S.-W. Tsao, K.-W. Cheah, K.-C. Lau, Y.-Y. Yang, J.-C. Chen and M. H.-W. Lam, *Inorg. Chem.*, 2009, **48**, 872–878.
7 P. Wu, E. L. Wong, D. Ma, G. S. Tong, K. Ng and C. Che, *Chem. – A Eur. J.*, 2009, **15**, 3652–3656.
8 K. Mitra, C. E. Lyons and M. C. T. Hartman, *Angew. Chemie Int. Ed.*, 2018, **57**, 10263–10267.
9 J. Wu, B. Xu, Y. Xu, L. Yue, J. Chen, G. Xie and J. Zhao, *Inorg. Chem.*, 2023, **62**, 19142–19152.
10 A. Upadhyay, A. Nepalia, A. Bera, D. K. Saini and A. R. Chakravarty, *Chem. – An Asian J.*, 2023, **18**, 1–11.
11 P. K. Chow, C. Ma, W. P. To, G. S. M. Tong, S. L. Lai, S. C. F. Kui, W. M. Kwok and C. M. Che, *Angew. Chemie - Int. Ed.*, 2013, **52**, 11775–11779.
12 M. Yoshida, K. Saito, H. Matsukawa, S. Yanagida, M. Ebina, Y. Maegawa, S. Inagaki, A. Kobayashi and M. Kato, *J. Photochem. Photobiol. A Chem.*, 2018, **358**, 334–344.
13 D. Gómez de Segura, A. Corral-Zorzano, E. Alcolea, M. T. Moreno and E. Lalinde, *Inorg. Chem.*, 2024, **63**, 1589–1606.
14 P. Domingo-Legarda, A. Casado-Sánchez, L. Marzo, J. Alemán and S. Cabrera, *Inorg. Chem.*, 2020, **59**, 13845–13857.
15 Y.-C. Wei, S. F. Wang, Y. Hu, L.-S. Liao, D.-G. Chen, K.-H. Chang,

C.-W. Wang, S.-H. Liu, W.-H. Chan, J.-L. Liao, W.-Y. Hung, T.-H. Wang, P.-T. Chen, H.-F. Hsu, Y. Chi and P.-T. Chou, *Nat. Photonics*, 2020, **14**, 570–577.
16 S.-F. Wang, B.-K. Su, X.-Q. Wang, Y.-C. Wei, K.-H. Kuo, C.-H. Wang, S.-H. Liu, L.-S. Liao, W.-Y. Hung, L.-W. Fu, W.-T. Chuang, M. Qin, X. Lu, C. You, Y. Chi and P.-T. Chou, *Nat. Photonics*, 2022, **16**, 843–850.
17 G. Cheng, P.-K. Chow, S. C. F. Kui, C.-C. Kwok and C.-M. Che, *Adv. Mater.*, 2013, **25**, 6765–6770.
18 Y. Yuan, J. L. Liao, S. F. Ni, A. K. Y. Jen, C. S. Lee and Y. Chi, *Adv. Funct. Mater.*, 2020, **30**, 1–8.
19 H. Yersin, *Highly Efficient OLEDs with Phosphorescent Materials*, Wiley, 2008.
20 K. Li, G. S. Ming Tong, Q. Wan, G. Cheng, W.-Y. Tong, W.-H. Ang, W.-L. Kwong and C.-M. Che, *Chem. Sci.*, 2016, **7**, 1653–1673.
21 P. Pander, R. Daniels, A. V. Zaytsev, A. Horn, A. Sil, T. J. Penfold, J. A. G. Williams, V. N. Kozhevnikov and F. B. Dias, *Chem. Sci.*, 2021, **12**, 6172–6180.
22 P. Pander, A. V. Zaytsev, A. Sil, J. A. G. Williams, P.-H. Lanoe, V. N. Kozhevnikov and F. B. Dias, *J. Mater. Chem. C*, 2021, **9**, 10276–10287.
23 P. Pander, A. V. Zaytsev, A. Sil, J. A. G. Williams, V. N. Kozhevnikov and F. B. Dias, *J. Mater. Chem. C*, 2022, **10**, 4851–4860.
24 H. Uoyama, K. Goushi, K. Shizu, H. Nomura and C. Adachi, *Nature*, 2012, **492**, 234–238.
25 Y. Tao, K. Yuan, T. Chen, P. Xu, H. Li, R. Chen, C. Zheng, L. Zhang and W. Huang, *Adv. Mater.*, 2014, **26**, 7931–7958.
26 A. Russegger, S. M. Fischer, A. C. Debruyne, H. Wiltsche, A. D. Boese, R. I. Dmitriev and S. M. Borisov, *ACS Appl. Mater. Interfaces*, 2024, **16**, 11930–11943.
27 F. Juliá, D. Bautista, J. M. Fernández-Hernández and P. González-Herrero, *Chem. Sci.*, 2014, **5**, 1875–1880.
28 R. J. Ortiz, J. D. Braun, J. A. G. Williams and D. E. Herbert, *Inorg. Chem.*, 2021, **60**, 16881–16894.
29 Y. M. Dikova, D. S. Yufit and J. A. G. Williams, *Inorg. Chem.*, 2023, **62**, 1306–1322.
30 S. J. Farley, D. L. Rochester, A. L. Thompson, J. A. K. Howard and J. A. G. Williams, *Inorg. Chem.*, 2005, **44**, 9690–9703.
31 F. Neese, *WIREs Comput. Mol. Sci.*, 2012, **2**, 73–78.
32 F. Neese, *WIREs Comput. Mol. Sci.*, , DOI:10.1002/wcms.1606.
33 M. Roemelt, D. Maganas, S. DeBeer and F. Neese, *J. Chem. Phys.*, 2013, **138**, 204101.
34 B. de Souza, G. Farias, F. Neese and R. Izsák, *J. Chem. Theory Comput.*, 2019, **15**, 1896–1904.
35 S. J. Strickler and R. A. Berg, *J. Chem. Phys.*, 1962, **37**, 814–822.
36 M. Urban, P. H. Marek-Urban, K. Durka, S. Luliński, P. Pander and A. P. Monkman, *Angew. Chemie - Int. Ed.*, , DOI:10.1002/anie.202217530.
37 P. Pander, A. V. Zaytsev, L. G. Franca, F. B. Dias and V. N. Kozhevnikov, *Inorg. Chem.*, 2023, **62**, 18465–18473.
38 P. Pander, A. V. Zaytsev, A. Sil, G. V. Baryshnikov, F. Siddique, J. A. G. Williams, F. B. Dias and V. N. Kozhevnikov, *Chem. Sci.*, 2023, **14**, 13934–13943.